Multiphonon dephasing of the 1086-cm^{-1} mode in calcite

P. J. Delfyett, R. Dorsinville, and R. R. Alfano
Institute for Ultrafast Spectroscopy and Lasers, Photonics Application Laboratory, Department of Electrical Engineering, The City College of New York, New York, New York 10031
(Received 7 March 1988)

The dephasing time of the 1086-cm^{-1} mode in calcite has been measured as a function of temperature using a new, innovative single-shot streak-camera technique that measures the phonon dephasing rate in *real time*. Phonon-phonon interaction models have been proposed and tested to explain the temperature dependence of the experimentally measured dephasing time. It is found that multiphonon splitting and scattering processes involving at least four phonons substantially contribute to the dephasing of the 1086-cm^{-1} mode in calcite.

INTRODUCTION

There has been considerable research devoted to the understanding of optical-phonon dynamics because of its importance to future high-speed-transport devices. Several techniques have been employed which give information about the phonon linewidth, phonon frequencies, dispersion relations, symmetry type, and phonon dephasing times.[1-8] Alfano and Shapiro[5,9] and Laubereau and co-workers[6,10] were the first to utilize picosecond laser pulses to coherently drive and directly measure the dephasing time of phonons in several solids and liquids. Over the years, several groups have performed similar experiments in GaP,[11,12] ZnSe,[13] diamond,[14] and quartz.[15] In all of the investigations the experimental technique relied on the picosecond excite-and-probe method to monitor the temporal evolution of the phonons. The temperature dependence of some of these dephasing processes were also investigated and attributed to three-phonon decay processes.

In this paper, a new innovative technique is employed to *measure directly* the phonon dephasing time of the 1086-cm^{-1} mode of calcite in *real time* as a function of temperature. The purpose of this work is twofold: to show that three-phonon anharmonic processes are not sufficient for describing the phonon dynamics of calcite, and to show that depopulation dynamics are mainly responsible for the coherent dephasing of phonons in calcite. The inclusion of four-phonon processes are necessary and have been included to describe the temperature dependence of the experimentally measured dephasing time in calcite.

EXPERIMENTAL METHOD

The experimental method for measuring coherent optical-phonon dephasing rates in real time utilizes Raman-induced phase-conjugation spectroscopy[16,17] (RIPS) and streak-camera technology. The laser pulses were obtained from a Quantel Nd:YAG (yttrium aluminum garnet) laser system. In this technique, two coherent laser pulses of frequency ω_1 and ω_2 are spatially and temporally coincident at 170° in a 1-cm calcite sample. This creates a coherently driven nonlinear polarization at the difference frequency $\omega_1-\omega_2=\Omega$, where Ω is the 1086-cm^{-1} phonon frequency. A third probing pulse at ω_1, traveling opposite to ω_2, interrogates the nonlinear polarization. This probe pulse is scattered from the nonlinear polarization into the phase-conjugate direction, and is shifted to ω_2. In practice, a broadband picosecond continuum pulse $\sim$2 psec in duration[18] is used as ω_2 which coherently drives all the Raman-active phonon modes that have frequencies which lie within the bandwidth of the continuum, $\sim$2500 cm^{-1}. Thus, the complete phase-matched Raman spectra can be obtained spanning thousands of wave numbers, with a single laser pulse.[17]

To measure the dephasing rate of the coherently excited phonons, the Raman-scattered phase-conjugate signal is appropriately filtered to select the desired Stokes frequency and is directed into a 2-psec Hamamatsu streak camera and computer video system. In the limit of a long probing pulse $\sim$30 psec, and a short pumping pulse $\sim$2 psec, the scattered RIPS pulse envelope varies as $\exp(-2t/\tau_\phi)$, where τ_ϕ is the dephasing time of the coherently driven phonons.[19] This technique was successfully tested by measuring the dephasing time of the 656-cm^{-1} mode in CS_2, which was measured to be 20 psec, in excellent agreement with previously measured dephasing times[20] and linewidth measurements.[21] The resolution limit of this technique was determined to be $\sim$2 psec by measuring the dephasing time of the 630-cm^{-1} mode in $LiNbO_3$,[19] which is known to have a subpicosecond response, from linewidth measurements.[22] In the current experiment, the 1086-cm^{-1} mode is spectrally seclected by inserting a 10-nm bandpass filter in the beam path of the Raman-scattered pulse, before entering the streak camera. In order to determine the temperature dependence of the dephasing time for this mode, the calcite sample was situated in a Janis optical helium Dewar with a temperature controller and thermocouple system. The RIPS spectra were simultaneously monitored using a Jarrell-Ash 1-m spectrometer and optical-multichannel-analyzer II system. The experiment was carried out by collecting several single-shot dephasing events and storing the data for later analysis. The temperatures at

which the experiment were performed, varied from 5 to 300 K.

EXPERIMENTAL RESULTS

At least 12 single-shot RIPS decay events were recorded for each temperature and averaged to eliminate noise fluctuations in the streak-camera output. Decay times of the RIPS signals were extracted from the averaged data, using a least-squares-fit algorithm. A typical RIPS pulse shape from the calcite sample at 10 K is shown in Fig. 1. The RIPS pulse envelope has been modeled to fit a single exponential with a dephasing time of 20 psec, which is shown by the dotted line.

The experimentally measured dephasing rates τ_ϕ^{-1} of the 1086-cm^{-1} A_{1g} mode in calcite are plotted as a function of temperature in Fig. 2. The salient feature in our data is a rapid rise in the dephasing rate for high temperatures. At low temperatures, less than 50 K, the experimentally measured dephasing time τ_ϕ of the phase conjugate signal is 20 psec. Above 50 K the decay rate of the phase-conjugate signal increases, gives a dephasing time τ_ϕ of 9 psec at room temperature.

THEORY

The phonons which are generated in this technique are coherent with a well-defined wave vector **k** and frequency Ω determined by two interacting laser pulses. The excess population in the excited mode **k** greatly exceeds the thermal equilibrium number, leading to a nonequilibrium phonon distribution. The phonon distribution function becomes a sharply peaked function in both momentum and energy space. The nonequilibrium distribution thermalizes to a boson distribution by dephasing along **k** and depopulation processes, leading to a direct loss of scattered light in the phase-matched direction.

The relative number of coherently excited phonons to the thermally excited phonons in a small range Δk can be easily estimated. The number of phonons generated is determined by the weaker of the two pumping beams, i.e., the continuum pulse. Assuming a 20-(nJ/nm) continuum pulse at the Stokes wavelength ($\lambda=564$ nm), a 1-mm^2 spot size, a 3-psec pulse duration, a 0.1% conversion efficiency to the generated phase-conjugate Raman signal, and a 1-cm^{-1} range of Δk, which corresponds to the linewidth at room temperature, the number of coherent phonons per cubic centimeter, N_{phonon}, is $\sim 10^9$. The density of excited optical-phonon modes can be obtained from the equation

$$N_{\text{modes}} = \frac{k^2_{\text{phonon}} \Delta k \Delta \Psi}{(2\pi)^3} , \tag{1}$$

where $k_{\text{phonon}} \sim 2k_{\text{laser}} \sim 2\times 10^4$, $\Delta k = 1$ cm^{-1}, and $\Psi = 10^{-4}$ sr. This leads to a density of excited modes equal to ~ 100 modes/cm^3. For comparison, the approximate total density of modes in the branch is $\sim 10^{22}$. The number of coherent optical phonons per mode which have been generated is then $N_{\text{phonon}}/N_{\text{modes}} \sim 10^7$ phonons/mode. Comparing this to the thermal equilibrium number at room temperature gives

$$N_{\text{thermal}} = \frac{1}{e^{\hbar\Omega/kT}-1} = 5\times 10^{-3} \text{ phonons/mode} , \tag{2}$$

leading to a thermally excited phonon density $N_{\text{thermal}} \times N_{\text{modes}} \sim 10^{-1}$ phonons/cm^3. This shows that the number of coherent phonons generated by the two interacting laser pulses greatly exceed the thermal phonon number in the mode $k \pm \Delta k$, the ratio of these two quantities being $\sim 10^{10}$. Calculating a temperature for the coherent population using these numbers, yields temperatures on the

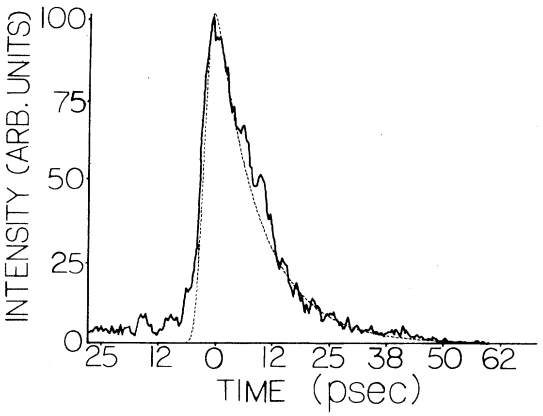

FIG. 1. The averaged RIPS pulse shape for the 1086-cm^{-1} mode of calcite at 10 K. The dotted curve corresponds to a full width at half maximum (FWHM) 3.5-psec Gaussian pulse convolved with an exponentially decaying impulse response with a dephasing time $\tau_\phi = 20$ psec.

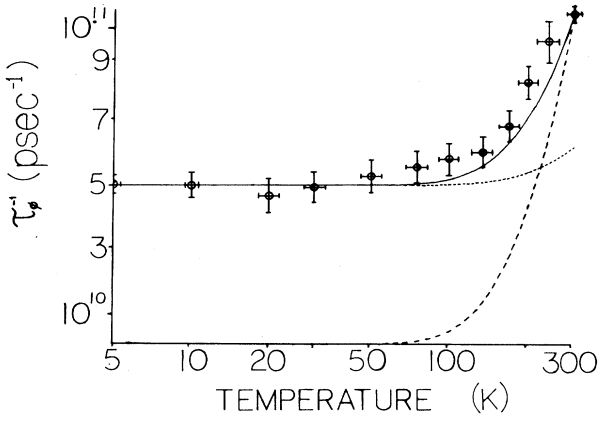

FIG. 2. Theoretical and experimentally measured dephasing rates τ_ϕ of the 1086-cm^{-1} mode of calcite plotted vs temperature. The dotted and dashed curves represent the decay rate for the three-phonon splitting and scattering processes, respectively. The solid curve represents the best fit for a combination of both processes. The fitting parameters were 0.528 and 1.77 cm^{-1} for the splitting and scattering processes, respectively. The vibrational frequencies used in the calculations are given in the text. The error in the experimentally measured decay times is 10%.

TABLE I. Direct-product table for the interaction of three phonons.

$\otimes$	A_{1g}	E_g	A_{2u}	E_u	A_{1u}	A_{2g}
A_{1g}	A_{1g}	E_g	A_{2u}	E_u	A_{1u}	A_{2g}
E_g		A_{1g}, E_g, A_{2g}	E_u	A_{1u}, A_{2u}, E_u	E_u	E_g
A_{2u}			A_{1g}	E_g	A_{2g}	A_{1u}
E_u				A_{1g}, A_{2g}, E_g	E_g	E_u
A_{1u}					A_{1g}	A_{2u}
A_{2g}						A_{1g}

order of 10^{10} K. This shows that the coherent optical-phonon distribution is non-boson-like. Information regarding the phonon dynamics in this regime of high excitation can only be obtained with direct time-resolved measurements.

Previous workers[6,12,13,15] have used three-phonon anharmonic processes to account for the observed temperature dependence of optical-phonon decay times. Higher-order multiphonon processes, involving at least four phonons, are necessary to account for the experimentally observed behavior in calcite. We will show in the following that the temperature dependence of the A_{1g} phonon decay rate can be modeled by using three- and four-phonon decay and scattering processes. These results indicate that other dephasing mechanisms, such as scattering from defects and impurities, do not play a significant role. As a result, the main dephasing mechanisms are attributed to depopulation.

Below, we incorporate the anharmonic processes which involves both the cubic and quartic terms of the interaction Hamiltonian. The quartic terms are mandatory and have been included for two reasons. (1) The Hamiltonian which results when only the cubic terms in the anharmonic interaction are retained leads to a system without a lowest-energy state, or ground state. This is a physically unrealistic situation. The inclusion of the quartic terms, however, circumvents this anomaly, and leads to a system with a ground state.[23,24] (2) The third-order processes which are governed by the cubic terms are often restricted by the stringent requirements imposed by the energy- and momentum-conservation laws. As a result, such a limited number of three-phonon processes may be allowed that the quartic terms can be of comparable importance and significantly contribute to the phonon dephasing rate.

Calcite belongs to the D_{3d} crystal class. The selection rules for cubic (three-) and quartic (four-) phonon interactions can be determined using standard group-theory methods.[25] For three-phonon decay events, the A_{1g} mode, being totally symmetric, will decay into two phonons of the same symmetry, i.e., $2E_u$, $2E_g$, $2A_{1u}$, $2A_{2u}$, $2A_{1g}$, $2A_{2g}$. Tables I and II show all of the allowed three- and four-phonon processes, which are given by the products of the irreducible representations of the D_{3d} group. There are six possible three-phonon decay paths allowed by symmetry, with another six possible three-phonon scattering processes, that involve the A_{1g} mode. In order to determine what processes actually exist, energy and momentum conservation must be maintained. A list of the known vibration modes at $k=0$ and their sym-

TABLE II. Direct-product table for the interaction of four phonons.

$\otimes$	A_{1g}	E_g	A_{2u}	E_u	A_{1u}	A_{2g}
$A_{1g}\otimes A_{1g}$	A_{1g}					
$A_{1g}\otimes E_g$	E_g					
$A_{1g}\otimes A_{2u}$	A_{2u}					
$A_{1g}\otimes E_u$	E_u					
$A_{1g}\otimes A_{1u}$	A_{1u}					
$A_{1g}\otimes A_{1u}$	A_{2g}					
$E_g\otimes E_g$	A_{1g}, A_{2g}, E_g	$E_g, E_g, E_g, A_{1g}, A_{2g}$				
$E_g\otimes A_{2u}$	E_u	A_{1u}, A_{2u}, E_u				
$E_g\otimes E_u$	A_{1u}, A_{2u}, E_u	$E_u, E_u, E_u, A_{1u}, A_{2u}$				
$E_g\otimes A_{1u}$	E_u	A_{1u}, A_{2u}, E_u				
$E_g\otimes A_{2g}$	E_g	A_{1g}, A_{2g}, E_g				
$A_{2u}\otimes A_{2u}$	A_{1g}	E_g	A_{2u}			
$A_{2u}\otimes E_u$	E_g	A_{1g}, A_{2g}, E_g	E_u			
$A_{2u}\otimes A_{1u}$	A_{2g}	E_g	A_{1u}			
$A_{2u}\otimes A_{2g}$	A_{1u}	E_u	A_{2g}			
$E_u\otimes E_u$	A_{1g}, A_{2g}, E_g	$E_g, E_g, E_g, A_{1g}, A_{2g}$	A_{1u}, A_{2u}, E_u	$E_u, E_u, E_u, A_{1u}, A_{2u}$		
$E_u\otimes A_{1u}$	E_g	A_{1g}, A_{2g}, E_g	E_u	A_{1u}, A_{2u}, E_u		
$E_u\otimes A_{2g}$	E_u	A_{1u}, A_{2u}, E_u	E_g	A_{1g}, A_{2g}, E_g		
$A_{1u}\otimes A_{1u}$	A_{1g}	E_g	A_{2u}	E_u	A_{1u}	
$A_{1u}\otimes A_{2g}$	A_{2u}	E_u	A_{1g}	E_g	A_{2g}	
$A_{2g}\otimes A_{2g}$	A_{1g}	E_g	A_{2u}	E_u	A_{1u}	A_{2g}

metry and dispersion is given in Table II.

Using the selection rules of Tables I and II and the vibrational frequencies listed in Table III show that only one three-phonon decay path exists:

$$A_{1g(1086)} = E_{u(715)} + E_{u(371)} , \tag{3a}$$

and only one three-phonon scattering process exists:

$$A_{1g(1086)} + E_{u(321)} = E_{u(1407)} . \tag{3b}$$

The splitting process described by Eq. (3a) will dominate at low temperatures due to the finite probability of a phonon splitting process occurring. The scattering process in Eq. (3b) has an infinitely long scattering time at low temperatures because of the requirement that a negligible phonon population exists at low temperatures. Thus, the scattering process will manifest itself only at high temperatures. The values used for the E_u mode above differ slightly from the $k=0$ values listed in Table II; however, these values fall within the allowed dispersion for this mode as displayed in Ref. 2. Conservation of momentum is easily satisfied because of the small dispersion in the 715- and 1407-cm^{-1} modes.

Four-phonon processes are needed because of the limited number of three-phonon decay and dephasing pathways. As a result, the higher-order phonon interactions substantially contribute to the phonon dephasing rate.

TABLE III. List of the symmetry type, vibrational frequencies, and range of dispersion for optical phonons in calcite, after Refs. 2, 3, 7, and 8. The value of the vibrational frequencies are given in units of wave numbers. The centered number in each box gives the value of the vibrational frequency at $k=0$. The lower numbers give the range of dispersion of the vibrational frequencies in the Brillouin zone.

Symmetry	Vib. freq.	Dispersion range
E_u	102	85–130
	123	123–150
	223	180–223
	239	
	297	290–310
	381	320–381
	715	
	1407	
	1549	
E_g	157	157–175
	287	230–300
	1434	
A_{2u}	92	90–130
	136	136–180
	303	
	387	
	875	870–890
A_{2g}	210	
	227	
A_{1u}	300	
A_{1g}	1086	

There are three types of four-phonon processes. The symmetry rules for the four-phonon processes can be obtained from Table II. The first type allows the coherent excited-state phonon to decay or split into three phonons of lower energy. For the A_{1g} mode, 13 possible decay paths exist. Of these 13 possibilities, only five conserve energy. These processes are

$$E_{g(712)} + E_{g(164)} + A_{2g(210)} = A_{1g} , \tag{4a}$$

$$E_{g(279)} + E_{u(715)} + A_{2u(92)} = A_{1g} , \tag{4b}$$

$$E_{g(271)} + E_{u(715)} + E_{u(102)} = A_{1g} , \tag{4c}$$

$$E_{g(712)} + E_{u(102)} + A_{1u(272)} = A_{1g} , \tag{4d}$$

$$E_{u(715)} + E_{u(94)} + A_{2g(277)} = A_{1g} . \tag{4e}$$

These processes have a finite probability of occurring, because they are of the splitting type, and therefore will dominate at low temperatures.

The second type of four-phonon process involves the interaction of a coherent excited-state phonon Ω_1 and a thermally produced phonon Ω_2. This interaction produces an intermediate state via the direct-product table, which then decays into two new phonons, Ω_3 and Ω_4, in accordance with the two-phonon direct-product table. For the A_{1g} mode there are 27 possible scattering mechanisms of this type allowed by symmetry considerations. The most common interaction of this type which satisfies energy and symmetry considerations is when $\Omega_1=\Omega_3$ and $\Omega_2=\Omega_4$, e.g.,

$$A_{1g(1086)} + A_{2u(92)} = A_{1g(1086)} + A_{2u(92)} . \tag{5}$$

This can be considered as a pure dephasing process. In this process, the phase of the phonons after the collision becomes interrupted and randomized with respect to the phase of the phonons before the collision. The probability of a phonon having a particular phase will be uniformly distributed between 0 and 2π, with a value $1/2\pi$. Thus there is no net loss in phonon number in the excited state, only a phase change in the vibrational oscillations before and after the collision. The reason for not considering interactions with acoustic phonons with frequencies less than ~ 75 cm^{-1} is because of the negligible density of states for these modes.[2] Since this process is a scattering process, it has an infinitely long dephasing rate at 0 K, and therefore will contribute only at high temperatures.

The third type of four-phonon process corresponds to a coherent excited-state phonon colliding with two thermally produced phonons to create a single phonon with a vibrational frequency equal to the sum of the three colliding phonons. A typical process of this type which satisfies energy and symmetry considerations is

$$A_{1g(1086)} + E_{g(160)} + E_{g(160)} = E_{g(1406)} . \tag{6}$$

The E_g modes at 160 cm^{-1} were chosen because these are the two modes of lowest vibrational frequencies that conserve energy in this process. These modes are more

densely populated at lower temperatures than the higher vibrational modes, and as a result should have the greatest effect on the dephasing as the temperature is increased. As we can see, there are many four-phonon pathways. Only a few are needed to fit the data.

The above processes account for the depopulation of the coherent excited phonon state. The exact reverse of these processes also occurs, and contributes to additional dephasing. For example, two thermally produced phonons can collide to produce a phonon in the excited state. This new phonon will not have the same phase as the coherent excited state. Thus, the loss of a coherent excited-state phonon via decay or scattering along with the simultaneous production of an incoherent excited-state phonon from the reverse process leaves the net population unchanged but introduces a phonon with a phase different from the coherent excited state. The overall effect reduces the coherency of the excited phonon state and thus can be considered as a dephasing process.

The dephasing time of the coherent phonons can be calculated from the inverse linewidth arising from multiphonon processes. The interaction Hamiltonian for the anharmonic processes is given by[26]

$$H_{\rm anh}=\frac{1}{3!}\sum_{\substack{a,b,c\\ l,l',l''}}^{l,l',l''}\Phi_{abc}^{ll'l''}u_a^l u_b^{l'}u_c^{l''}+\frac{1}{4!}\sum_{\substack{a,b,c,d\\ l,l',l'',l'''}}\Phi_{abcd}^{ll'l''l'''}u_a^l u_b^{l'}u_c^{l''}u_d^{l'''}+\cdots , \tag{7}$$

where the summation is over all atoms and their corresponding displacements from the equilibrium position. Transforming to the normal coordinate representation to eliminate cross-terms in the products of the displacements using

$$u_a^l=\epsilon(la;\mathbf{k}j)q(\mathbf{k}j) \tag{8}$$

gives

$$H_{\rm anh}=\frac{1}{3!(mN)^{3/2}}\sum_{\substack{a,b,c\\ l,l',l''}}\Phi_{abc}^{ll'l''}e_a(\mathbf{k}_1,j_1)e_b(\mathbf{k}_2,j_2)e_c(\mathbf{k}_3,j_3)q(\mathbf{k}_1,j_1)q(\mathbf{k}_2,j_2)q(\mathbf{k}_3,j_3)e^{-i(\mathbf{k}_1\cdot\mathbf{r}^l+\mathbf{k}_2\cdot\mathbf{r}^{l'}+\mathbf{k}_3\cdot\mathbf{r}^{l''})}$$
$$+\frac{1}{4!(mN)^2}\sum_{\substack{a,b,c,d\\ l,l',l'',l'''}}\Phi_{abcd}^{ll'l''l'''}e_a(\mathbf{k}_1,j_1)e_b(\mathbf{k}_2,j_2)e_c(\mathbf{k}_3,j_3)e_d(\mathbf{k}_4,j_4)$$
$$\times q(\mathbf{k}_1,j_1)q(\mathbf{k}_2,j_2)q(\mathbf{k}_3,j_3)q(\mathbf{k}_4,j_4)e^{-i(\mathbf{k}_1\cdot\mathbf{r}^l+\mathbf{k}_2\cdot\mathbf{r}^{l'}+\mathbf{k}_3\cdot\mathbf{r}^{l''}+\mathbf{k}_4\cdot\mathbf{r}^{l'''})}+\cdots . \tag{9}$$

In the above equations, $\epsilon(l\alpha,\mathbf{k}j)$ is the transformation matrix given by

$$\frac{1}{(mN)^{1/2}}e_a(\mathbf{k},j)e^{-i\mathbf{k}\cdot\mathbf{r}} \tag{10}$$

and $e(\mathbf{k},j)$ is the polarization vector corresponding to a particular phonon with a wave vector $\mathbf{k}$ and mode j. The $q(\mathbf{k},j)$ terms can be given by the creation and annihilation operators $a^\dagger$ and a;

$$q(\mathbf{k}_i,j_i)=\left[\frac{\hbar}{2\Omega(\mathbf{k}_i,j_i)}\right]^{1/2}[a^\dagger(-\mathbf{k}_i,j_i)+a(\mathbf{k}_i,j_i)] . \tag{11}$$

The anharmonic Hamiltonian is then written as

$$H_{\rm anh}=\frac{1}{3!}\sum_{\substack{a,b,c\\ l,l',l''}}\Phi_{abc}^{ll'l''}e(\mathbf{k}_1,j_1)e(\mathbf{k}_2,j_2)e(\mathbf{k}_3,j_3)(a_1^\dagger+a_1)(a_2^\dagger+a_2)(a_3^\dagger+a_3)\exp[-i(\mathbf{k}_1\cdot\mathbf{r}^l+\mathbf{k}_2\cdot\mathbf{r}^{l'}+\mathbf{k}_3\cdot\mathbf{r}^{l''}]$$
$$+\frac{1}{4!}\sum_{\substack{a,b,c,d\\ l,l',l'',l'''}}\Phi_{abcd}^{ll'l''l'''}e(\mathbf{k}_1,j_1)e(\mathbf{k}_2,j_2)e(\mathbf{k}_3,j_3)e(\mathbf{k}_4,j_4)(a_1'+a_1)(a_2^\dagger+a_2)(a_3^\dagger+a_3)(a_4^\dagger+a_4)$$
$$\times\exp[-i(\mathbf{k}_1\cdot\mathbf{r}^l+\mathbf{k}_2\cdot\mathbf{r}^{l'}+\mathbf{k}_3\cdot\mathbf{r}^{l''}+\mathbf{k}_4\cdot\mathbf{r}^{l'''})]+\cdots . \tag{12}$$

The calculation of the linewidth based on standard perturbation methods are often complicated and tedious. It is more convenient to make this calculation using Green's-function techniques[27] or by Klemens' analysis.[28,29] For three-phonon processes of the type discussed, the linewidth is given by[26,27,30]

$$\Gamma_3(\mathbf{k}_1,j_1;\Omega_1,T)=18\frac{\pi}{h^2}\sum_{\mathbf{k}_2,j_2}\sum_{\mathbf{k}_3,j_3}|V(\mathbf{k}_1,j_1;\mathbf{k}_2,j_2;\mathbf{k}_3,j_3)|^2\Delta(\mathbf{k}_1+\mathbf{k}_2+\mathbf{k}_3)$$
$$\times\{(1+\bar{n}_2+\bar{n}_3)[\delta(\Omega_1-\Omega_2-\Omega_3)-\delta(\Omega_1+\Omega_2+\Omega_3)]$$
$$+(\bar{n}_2-\bar{n}_3)[\delta(\Omega_1+\Omega_2-\Omega_3)-\delta(\Omega_1-\Omega_2+\Omega_3)]\} . \tag{13}$$

The quartic contribution to the linewidth can be calculated using similar techniques. It is given by

$$\Gamma_{(4)}(\mathbf{k}_1,j_1;\Omega_1,T)=96\frac{\pi}{h^2}\sum_{\mathbf{k}_2,j_2}\sum_{\mathbf{k}_3,j_3}\sum_{\mathbf{k}_4,j_4}|V(\mathbf{k}_1,j_1;\mathbf{k}_2,j_2;\mathbf{k}_3,j_3;\mathbf{k}_4,j_4)|^2\,\Delta(\mathbf{k}_1+\mathbf{k}_2+\mathbf{k}_3+\mathbf{k}_4)$$
$$\times\{(1+\bar{n}_2+\bar{n}_3+\bar{n}_4+\bar{n}_2\bar{n}_3+\bar{n}_2\bar{n}_4+\bar{n}_3\bar{n}_4)$$
$$\times[\delta(\Omega_1-\Omega_2-\Omega_3-\Omega_4)-\delta(\Omega_1+\Omega_2+\Omega_3+\Omega_4)]$$
$$+[\bar{n}_2(1+\bar{n}_3+\bar{n}_4)-\bar{n}_3\bar{n}_4][\delta(\Omega_1+\Omega_2-\Omega_3-\Omega_4)-\delta(\Omega_1-\Omega_2+\Omega_3+\Omega_4)]$$
$$+[\bar{n}_2\bar{n}_3-\bar{n}_4(1+\bar{n}_2+\bar{n}_3)][\delta(\Omega_1+\Omega_2+\Omega_3-\Omega_4)-\delta(\Omega_1-\Omega_2-\Omega_3+\Omega_4)]\}\,, \tag{14}$$

where n_i is the mean occupation number of phonons of the type k_i , j_i, and phonon frequency Ω_i. The $\Delta(\cdots)$ allows for phase matching of the phonons, or momentum conservation. In the above equations the V's are complicated functions which contain the information about the anharmonic coupling coefficients, phonon polarization vectors, atomic masses, and normal-mode frequencies.

DISCUSSION

The temperature dependence of the dephasing time due to three-phonon processes can be obtained from Eq. (13). The first two terms in Eq. (13) yields

$$\tau_{\phi_3}^{-1}(T)=\gamma_1(\bar{n}_2+\bar{n}_3+1) \tag{15}$$

for the splitting process, and

$$\tau_{\phi_3}^{-1}(T)=\gamma_2(\bar{n}_2-\bar{n}_3) \tag{16}$$

for the scattering process, where n_i is the thermal equilibrium population of the ith phonon vibration $n_i=[\exp(h\Omega/kT)-1]^{-1}$ and T is the temperature of the lattice.

In Fig. 2 the phonon decay rate of these processes are plotted versus temperature along with the experimental data, for comparison. The vibrational frequencies which were used in Eqs. (15) and (16) correspond to those given in Eqs. (3a) and (3b), respectively. From this figure we see that the three-phonon splitting process is nearly independent of temperature and can only fit the low-temperature data by properly adjusting γ, while the three-phonon scattering process highly dependent on temperature and can only if the high-temperature data. A combination of these processes is more realistic since it includes additional depopulation and dephasing mechanisms. This model gives a reasonable fit to the experimental data. This fit was obtained by using a least-squares algorithm. Large weighting factors were used in this algorithm at the 5- and 300-K data points. The parameter γ_1 is adjusted to fit the low-temperature data. Increasing amounts of γ_2 were added to minimize the error. The fitting parameters in this case were 0.528 and 1.77 cm^{-1} for the splitting and scattering processes, respectively. The reason for pinning the theoretical curve at these two points is as follows: At temperatures less than 40 K, the dephasing rate is constant. A large weighting factor at 5 K causes the theory to pass through the low-temperature data points. This minimizes the error at low temperatures. The large weighting factor at 300 K is used because this point has been previously measured by Refs. 1, 6, 19, and 31, and the results obtained by these investigators are in excellent agreement.

The contribution to the temperature dependence of the dephasing time arising from the four-phonon splitting process is given by the first term in Eq. (14). Using the procedures mentioned above yields

$$\tau_{\phi_4}^{-1}(T)=\gamma_3(1+\bar{n}_2+\bar{n}_3+\bar{n}_4+\bar{n}_2\bar{n}_4+\bar{n}_3\bar{n}_4+\bar{n}_2\bar{n}_3)\,, \tag{17}$$

where the n_i $(i=2,3,4)$ are the three-phonon states produced by the decay of the A_{1g} mode. The decay rate for these processes is plotted as a function of temperature in Figs. 3(a)–3(d). These processes all have the same salient features of a constant decay rate at low temperatures and a rapidly increasing decay rate going towards higher temperatures. The four-phonon splitting process clearly shows the same type of temperature dependence observed in the data. The vibrational frequencies used in Eq. (17) and displayed in Figs. 3(a)–3(d) correspond to Eqs. (4a)–4(d), respectively. The fitting parameter for these curves is 0.528 cm^{-1}.

The temperature dependence of the dephasing time for the four-phonon scattering process described by Eq. (5) is given by considering the second term of Eq. (14), which leads to a dephasing rate of

$$\tau_{\phi_4}^{-1}(T)=\gamma_4[\bar{n}_2(1+\bar{n}_3+\bar{n}_4)-\bar{n}_3\bar{n}_4]\,. \tag{18}$$

In this equation n_2 is one of the incoming phonons and n_3 and n_4 are the outgoing phonons. For pure dephasing, $\Omega_1=\Omega_3$ and $\Omega_2=\Omega_4$. The temperature dependence for this process is plotted in Fig. 4. The coherent excited-state phonon and the thermally produced phonon used in this calculation have vibrational frequencies of 1086 and 92 cm^{-1}, respectively. The fitting parameter used for this calculation is 0.217 cm^{-1}. The plot in Fig. 4 shows that for these phonons this type of four-phonon interaction can model the high-temperature data, but not the low-temperature data.

The temperature dependence of the dephasing time due to the third type of four-phonon interaction described by Eq. (6) is given by

$$\tau_{\phi_4}^{-1}(T)=\gamma_5[\bar{n}_2\bar{n}_3-\bar{n}_4(1+\bar{n}_2+\bar{n}_3)]\,. \tag{19}$$

In this equation n_2 and n_3 are the population of incoming

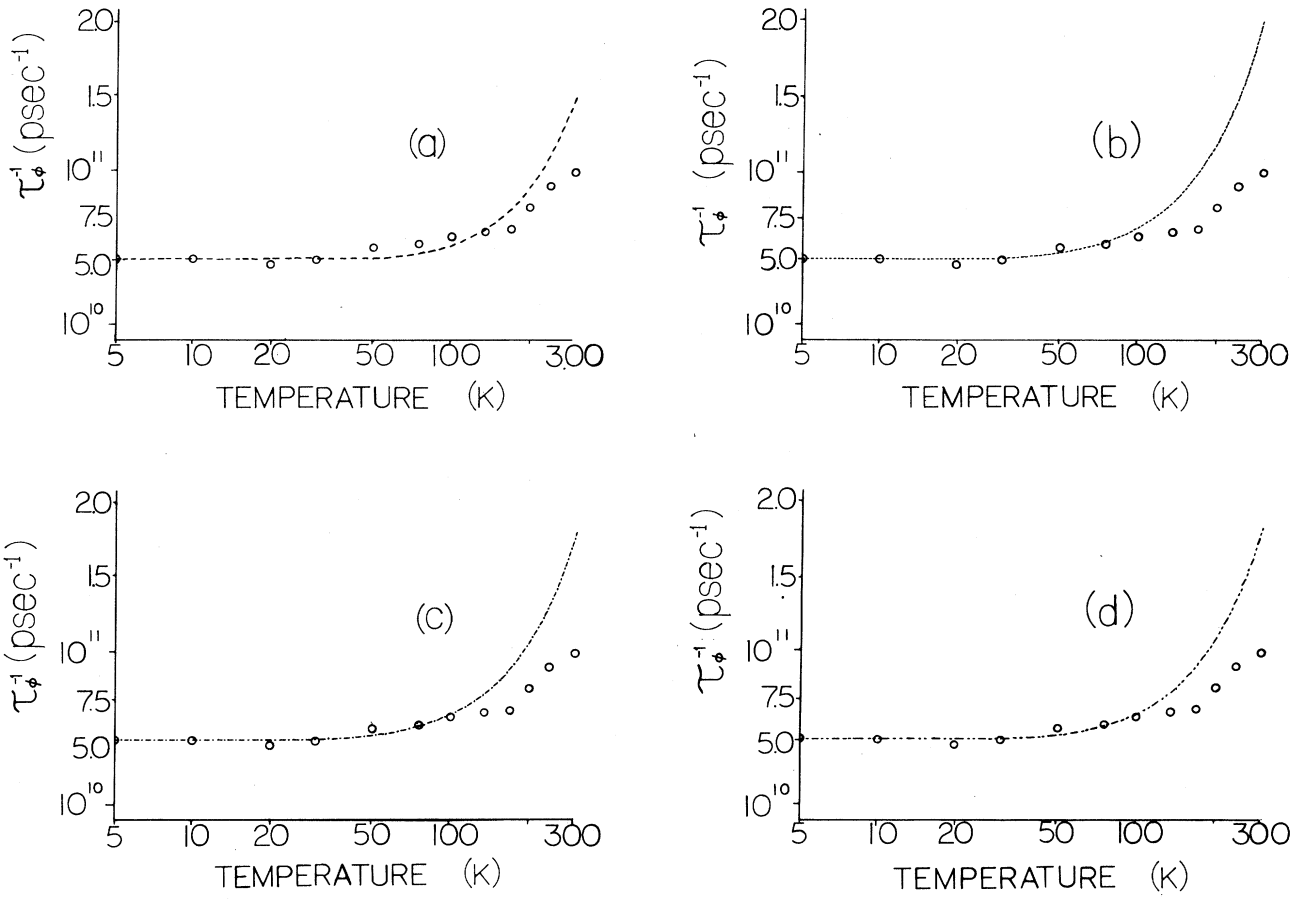

FIG. 3. Theoretical contribution to the four-phonon dephasing rate τ_ϕ^{-1} due to splitting. The experimental data are also shown for comparison. Panels (a)–(d) correspond to Eqs. 4(a)–4(d), respectively. The fitting parameter γ was chosen to be 0.528 cm^{-1} for these four interactions.

phonons and n_4 is the population of the outgoing phonon. Plotting the decay rate versus temperature for this type of four-phonon scattering process in Fig. 4 shows that this mechanism can account for the high-temperature regime of the experimental data, but cannot explain the low-temperature data. The vibrational frequencies of the two thermally produced incoming phonons were 160 cm^{-1} each, with a fitting parameter of 1.5 cm^{-1}. From the five types of models proposed, the process which most closely resembles the experimental data is that of four-phonon decay.

The phonon decay dynamics combine all three- and four-phonon processes discussed above, because the total dephasing is given by the inverse linewidth in Eqs. (13) and (14), which is a sum of all the allowed processes. It is apparent that a combination of a three-phonon decay process with any of the other processes discussed will, in fact, give a qualitative fit to the experimental data. With this in mind, a combination of the different types of decay and scattering models were investigated. The combination of processes which gives the best fit to the experimental data is a combination of a three- and a four-

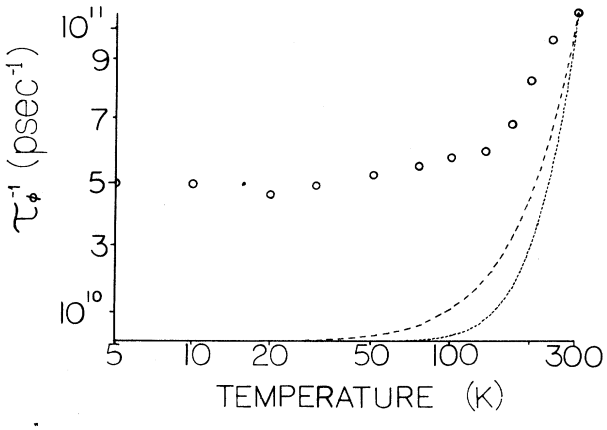

FIG. 4. Experimental results with the theoretical contribution to the four-phonon dephasing rate τ_ϕ^{-1} due to scattering. The vibrational frequencies and fitting parameters are given in the text. The dashed and dotted curves represent the pure dephasing processes and the second type of four-phonon scattering discussed in the text, i.e., Eqs. (5) and (6), respectively.

phonon splitting process. In Fig. 5 we show a combination of the three- and four-phonon decay mechanisms, which gives an excellent fit to the experimentally measured dephasing times. This fit was obtained using the same algorithm as in Fig. 2. The parameters γ_1 and γ_3 were adjusted such that the sum of γ_1 and γ_3 determines the low-temperature regime of the data while simultaneously minimizing the error. The vibrational frequencies which were used in this calculation correspond to Eqs. (3a) and (4a). The fitting parameters which give the best fit are 0.268 and 0.260 cm^{-1}, for the three- and four-phonon splitting processes, respectively.

A goodness-of-fit parameter can be calculated in the least-squares sense. The total squared error for the three-phonon decay and scattering processes (solid curve in Fig. 2) as compared with the data is 0.04. The total squared error for the three- and four-phonon decay processes (Fig. 5) is 0.032. This represents a 20% reduction of the error between the data and theoretical models when the three- and four-phonon decay models are used.

Another important feature of the three- and four-phonon decay model is that it accurately predicts the dephasing time for temperatures beyond the range investigated in our work. Our model predicts a dephasing time of ~ 3 psec at 700 K, which is in excellent agreement with the measured linewidth, ~ 3.5 cm^{-1}.[1] Using the model depicted in Fig. 2, which uses only three-phonon processes, predicts a dephasing time of ~ 4 psec at 700 K.

An important feature is obtained from this analysis. The four-phonon contribution contributes equally, with respect to the three-phonon contribution. However, since there are five allowed four-phonon splitting paths with roughly the same size coupling coefficient with the same qualitative temperature behavior which occur simultaneously, the total four-phonon splitting contribution is divided up among the five pathways. The four-phonon fitting parameter therefore represents a lumped anharmonic coefficient. The three-phonon splitting contribution is due to only one path, so its fitting parameter represents the anharmonic coefficient directly. With this in mind, the ratio of the quartic anharmonic coefficient to the cubic coefficient is $\gamma_3/5\gamma_1=0.19$, showing that the quartic terms are significant.

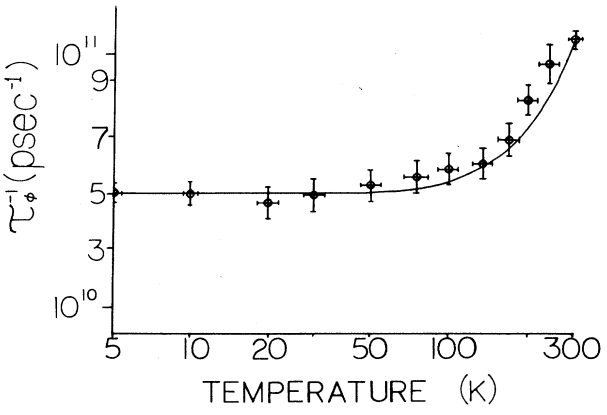

FIG. 5. The solid curve represents the phonon dephasing rate τ_ϕ^{-1} due to a combination of the three-phonon splitting processes and the four-phonon splitting processes. The vibrational frequencies used for the three- and four-phonon splitting processes are given by Eqs. (3a) and (4a), respectively. The fitting parameters are given in the text. The error in the experimentally measured decay times is 10%. This combination gives the best fit to our experimentally measured decay times.

Our work shows the following. (1) Depopulation dynamics is mainly responsible for the coherent dephasing of the 1086-cm^{-1} optical-phonon mode in calcite. At low temperatures, the dephasing is dominated by splitting processes, due to the finite dephasing rate at low temperatures, while at high temperatures the scattering processes become significant. (2) The combination of the three-phonon splitting process with any other process gives qualitative agreement with the experimental data. This implies that the three-phonon splitting process is the most dominant process. (3) A combination of both three- and four-phonon splitting processes were found to give the best fit to the data. This combination of processes involves only splitting processes, which implies that splitting contributes more to the dephasing, as compared to the scattering, for the temperature range investigated. (4) In addition, the different combinations of three- and four-phonon processes show that the addition of a four-phonon splitting mechanism to the three-phonon splitting process gives a better account of the system than the addition of the three-phonon scattering mechanism. This shows that four-phonon processes are necessary to explain the experimental data. The total quartic anharmonic coefficient is significant for the dephasing of optical phonons. This coupling coefficient is as large as the three-phonon process, and as a result both processes have similar transition rates and contribute equally to the relaxation processes. (5) The model depicted in Fig. 4 accurately predicts the dephasing rate at temperatures higher than what was investigated in this work.

CONCLUSION

In conclusion, we have measured the temperature dependence of the dephasing time of the 1086-cm^{-1} mode of calcite, in real time, using a single laser pulse. The temperature dependence of the dephasing time has been fitted to a theory involving both three- and four-phonon interactions. We have found that the four-phonon contribution must be included to explain the temperature dependence of the dephasing time. This mechanism also contributies as much as the three-phonon terms. As a result, the four-phonon interactions which arise from the quartic terms in the expression for the anharmonic Hamiltonian should not be neglected when the phonon dynamics of the 1086-cm^{-1} mode of calcite is being considered.

ACKNOWLEDGMENTS

We thank J. Birman and K. Arya for helpful discussions on phonon decay. This work was supported by the U.S. Air Force Office for Scientific Research (AFOSR) under Grant No. 86 0031.

[1]K. Park, Phys. Lett. **25A**, 490 (1967).
[2]M. Plihal and G. Schaack, Phys. Status Solidi **42**, 485 (1970).
[3]M. Plihal, Phys. Status Solidi B **56**, 495 (1973).
[4]S. P. S. Porto, J. A. Giordmaine, and T. C. Damen, Phys. Rev. **147**, 147 (1966).
[5]R. Alfano and S. Shapiro, Phys. Rev. Lett. **20**, 1247 (1971).
[6]A. Laubereau, G. Wochner, and W. Kaiser, Opt. Commun. **14**, 75 (1975).
[7]E. R. Cowley, A. K. Pant, Phys. Rev. B **8**, 4795 (1973).
[8]K. H. Hellwege, W. Lesch, M. Plihal, and G. Schaack, Z. Phys. **232**, 61 (1970).
[9]R. R. Alfano and S. L. Shapiro, Phys. Rev. Lett. **29**, 1655 (1972).
[10]A. Laubereau and W. Kaiser, Rev. Mod. Phys. **50**, 607 (1978).
[11]A. Laubereau, D. von der Linde, and W. Kaiser, Opt. Commun. **7**, 173 (1973).
[12]J. Kuhl and W. Bron, Soild State Commun **49**, 935 (1984).
[13]W. E. Bron, in *Nonequilibrium Phonon Dynamics,* Vol. 124 *of NATO Advanced Study Institute, Series B: Physics,* edited by W. E. Bron (Plenum, New York, 1985).
[14]A. Laubereau, D. von der Linde, and W. Kaiser, Phys. Rev. Lett. **27**, 802 (1971).
[15]G. Gale and A. Laubereau, Opt. Commun. **44**, 273 (1983).
[16]S. K. Saha and R. W. Hellwarth, Phys. Rev. A **27**, 919 (1983).
[17]R. Dorsinville, P. J. Delfyett, and R. R. Alfano, Appl. Opt. **26**, 3655 (1987).
[18]R. Dorsinville, P. J. Delfyett, and R. R. Alfano, Appl. Opt. **27**, 16 (1988).
[19]P. J. Delfyett, R. Dorsinville, and R. R. Alfano, Opt. Lett. **12**, 1002 (1987).
[20]J. P. Heritage, Appl. Phys. Lett. **34**, 470 (1979).
[21]W. R. L. Clements, and X. Stoicheff, Appl. Phys. Lett. **12**, 246 (1968).
[22]A. S. Barker and R. Loudon, Phys. Rev. **158**, 433 (1961).
[23]*Solid State Physics,* edited by N. W. Ashcroft and D. Mermin (Holt, Rinehart and Winston, New York, 1976).
[24]G. Baym, Phys. Rev. **117**, 886 (1960).
[25]G. Herzberg, *Molecular Spectra and Molecular Structure* (Van Nostrand, New York, 1945), Vol. II.
[26]J. A. Reissland, *The Physics of Phonons* (Wiley-Interscience, New York, 1973).
[27]M. Balkanski, R. F. Wallis, and E. Haro, Phys. Rev. B **28**, 1928 (1983).
[28]P. G. Klemens, Phys. Rev. **148**, 845 (1966).
[29]P. G. Klemens, Phys. Rev. **122**, 443 (1961).
[30]P. Breusch, *Phonons: Theory and Experiment I,* Vol. 34 of *Springer Series in Solid State Science* (Springer-Verlag, Berlin, 1982).
[31]T. Juhasz, J. S. Bakos, and C. S. Kuti, Phys. Status Solidi B **135**, K99 (1986).